

Criticality and Phase Structures of Excited Holographic Superconductors in Nonlinear Electrodynamics

Hoang Van Quyet

Department of Physics, Hanoi Pedagogical University 2, Xuan Hoa, Phu Tho, Vietnam

Abstract

We investigate the critical properties and phase structure of excited states in a holographic superconductor model within the framework of Varying Central Charge Thermodynamics, where the cosmological constant serves as a fundamental parameter controlling the number of degrees of freedom in the boundary conformal field theory. Employing Born-Infeld nonlinear electrodynamics, we explore how the nonlinear parameter b affects the condensation of the ground state (GS) and the two lowest excited states (ES1, ES2) in the background of a spherically symmetric Schwarzschild-AdS black hole. A state is classified as possessing a **hard gap** if its optical conductivity exhibits $\text{Re}\sigma(\omega) = 0$ for $\omega < \omega_g$, indicating a hard energy gap in the excitation spectrum and the Meissner effect. In contrast, a **gapless superconductor** possesses a non-zero order parameter but lacks a hard gap, with $\text{Re}\sigma(\omega) \neq 0$ as $\omega \rightarrow 0$. Our central finding reveals that the emergence of gapless phases in the excited states represents a genuine physical phenomenon arising from the competition between Born-Infeld nonlinear screening effects and the spatial curvature of the black hole geometry, not from numerical artifacts. Specifically, when the pressure P exceeds the critical pressure P_c , both GS and ES1 are gapped superconductors with hard energy gaps while ES2 is a gapless superconductor. However, when $P \leq P_c$, only GS remains gapped while both ES1 and ES2 condense into gapless phases. This curvature-controlled switching of superconducting properties provides a novel mechanism for engineering gapless superconductivity in strongly coupled systems through variation of the boundary CFT degrees of freedom, with potential implications for understanding unconventional high-temperature superconductors.

Keywords: Holographic superconductors, Excited states, Nonlinear electrodynamics, Varying Central Charge, Phase transitions, Spherical AdS black holes, Gapless superconductivity

1. Introduction

The AdS/CFT correspondence, discovered by Maldacena in 1997, has provided a profound theoretical framework for studying strongly coupled systems in condensed matter physics through gravitational duals [1, 2, 3]. One of the most successful applications of this duality is the holographic superconductor model, first constructed by Gubser [4] and Hartnoll, Herzog, and Horowitz [5, 6]. These authors demonstrated that a charged scalar field

Email address: hoangvanquyet@hpu2.edu.vn (Hoang Van Quyet)

can condense below a critical temperature T_c in AdS space with a black hole, and this phenomenon can be identified with high-temperature superconductivity in the boundary field theory. The holographic superconductor has become a paradigm for understanding strongly coupled superconductivity through the gauge/gravity duality [7, 8, 9, 10].

Most holographic superconductor models have been studied in the probe limit, where the matter fields do not affect the background geometry. In this approach, the background metric is fixed as a Schwarzschild-AdS or Reissner-Nordstrom-AdS black hole, and one solves for the dynamics of the charged scalar and gauge fields. The condensation of the scalar field gives rise to a superconducting gap in the dual field theory [11, 12].

In recent years, the development of black hole thermodynamics in the extended phase space has opened new frontiers connecting gravity and condensed matter physics [13, 14, 15, 16, 17, 18]. In this framework, the cosmological constant Λ is treated as a thermodynamic variable, with pressure defined as $P = -\Lambda/8\pi = 3/(8\pi L^2)$. The spherical Schwarzschild-AdS black hole geometry admits two thermodynamic branches—small and large black holes—that undergo a phase transition analogous to the van der Waals liquid-gas transition at a critical pressure P_c [13]. This small-to-large black hole phase transition has become a central tool for understanding critical phenomena in holographic dual field theories.

A crucial development in understanding the physical meaning of extended phase space thermodynamics was provided by Visser [19], who showed that the cosmological constant controls the number of degrees of freedom in the boundary theory through the holographic dictionary: $\Lambda \propto -1/L^2$ and $C \sim L^2/G_N$ (the Central Charge). This understanding was further refined by Ahmed, Cong, Kubiznak, Mann, and Visser [20], who formulated the holographic first law exactly dual to extended black hole thermodynamics with variable cosmological constant. Within this Varying Central Charge framework, which is equivalent to the **Central Charge Ensemble** approach, varying the pressure P in our calculations corresponds to transitioning between different boundary CFTs with varying Central Charges C (or equivalently, varying the number of colors N in Yang-Mills theory), while keeping the boundary volume \mathcal{V} fixed. This interpretation is essential for distinguishing our bulk thermodynamic pressure from any boundary pressure [19, 20]. This framework allows us to investigate the robustness of superconducting states—particularly the excited states—as the microscopic structure of the boundary theory changes.

Another important direction in holographic superconductors is the study of excited states [21, 22, 23, 24]. While most previous works focused exclusively on the ground state, recent studies have demonstrated that excited states—characterized by nodes in the scalar field radial profile—can participate in phase transitions. The number of accessible excited states depends on the chemical potential μ ; for example, $\mu = 4.064$ admits only the ground state, while $\mu = 35$ allows up to six excited states. Excited states in holographic superconductors have been studied in various contexts, including regularized Maxwell theory [24], higher-dimensional generalizations [25], and superfluid models with nonlinear electrodynamics [26]. However, the combined effects of Varying Central Charge (pressure) and Born-Infeld nonlinearity on excited states remain unexplored.

To address this gap, in the present work we incorporate Born-Infeld nonlinear electrodynamics [27] in the background of a spherically symmetric Schwarzschild-AdS black hole. Born-Infeld electrodynamics provides a natural extension of Maxwell theory with a finite maximum field strength, where the parameter b controls the nonlinearity. In the limit

$b \rightarrow 0$, standard Maxwell electrodynamics is recovered. Born-Infeld electrodynamics has found applications from string theory to condensed matter physics [28, 29], and investigating its effects on excited states in the Varying Central Charge framework is both timely and important.

Our spherically symmetric setup is essential for capturing the small-to-large black hole phase transition, which is absent in the planar (Rindler) slicing commonly used in holographic superconductors. The metric function $f(r) = 1 - 2M/r + r^2/L^2$ with positive curvature $k = 1$ leads to a cubic horizon equation with two positive real roots (small and large branches), enabling the rich phase structure we investigate.

The main objective of this paper is to explore how the triplet of holographic phase transitions (GS, ES1, ES2) responds to variations in pressure P and nonlinearity b . Our central finding reveals a pressure-dependent switching of superconducting properties: at $P > P_c$, both GS and ES1 are gapped superconductors with hard energy gaps while ES2 is a gapless superconductor; at $P \leq P_c$, only GS remains gapped while ES1 and ES2 become gapless phases. This non-trivial behavior arises from the competition between Born-Infeld screening effects and black hole geometric deformation induced by curvature, representing a novel mechanism for gapless superconductivity in strongly coupled systems. Importantly, we provide a physical explanation based on **energy density localization**: the ground state has its energy density concentrated near the black hole horizon, while excited states have wavefunctions with nodes extending to larger radii. When the black hole transitions from small to large (as P varies), the geometric deformation propagates outward and most strongly affects the extended wavefunctions of excited states, causing their hard energy gaps to close while the compactly supported ground state remains robustly gapped. This phenomenon, which we term **Nodal Structure Vulnerability**, provides a deep physical insight into the hierarchy of gap behaviors observed in our calculations.

The structure of this paper is as follows. In Section 2, we present the holographic setup with Born-Infeld electrodynamics in the Varying Central Charge framework using the spherical Schwarzschild-AdS black hole geometry. Section 3 is devoted to the equations of motion and numerical procedure. The numerical results are presented in Section 4, including critical temperature dependence, phase structure analysis, and conductivity properties. Section 5 provides a deep physical discussion of the triplet phenomenon and its implications. Finally, Section 6 summarizes our findings and discusses connections to real high-temperature superconductors and possible extensions.

2. Holographic Setup: Central Charge Ensemble with Spherical Geometry

We consider the action of a charged complex scalar field coupled to a gauge field in four-dimensional AdS space with spherical spatial sections. In the Born-Infeld nonlinear electrodynamics framework, the total action takes the form [28, 29]

$$S = \int d^4x \sqrt{-g} \left[\frac{1}{16\pi G} (R - 2\Lambda) + \mathcal{L}_{BI}(F) - |D_\mu \psi|^2 - m^2 |\psi|^2 \right], \quad (1)$$

where G is the gravitational constant, $\Lambda = -3/L^2$ is the negative cosmological constant (with L being the AdS radius), and $D_\mu = \partial_\mu - iqA_\mu$ is the covariant derivative with q being

the charge of the scalar field. The complex scalar field ψ has mass m , and A_μ is the gauge field.

The Born-Infeld Lagrangian is given by [27]

$$\mathcal{L}_{BI}(F) = \frac{1}{b^2} \left(1 - \sqrt{1 + \frac{b^2 F_{\mu\nu} F^{\mu\nu}}{2}} \right), \quad (2)$$

where b is the Born-Infeld nonlinear parameter. In the limit $b \rightarrow 0$, the Taylor expansion yields

$$\mathcal{L}_{BI}(F) = -\frac{1}{4} F_{\mu\nu} F^{\mu\nu} + \frac{b^2}{16} (F_{\mu\nu} F^{\mu\nu})^2 + \mathcal{O}(b^4), \quad (3)$$

recovering standard Maxwell electrodynamics. The parameter b has dimensions of inverse field; in our numerical calculations, we set b in appropriate units.

We employ the spherically symmetric Schwarzschild-AdS black hole metric [13]

$$ds^2 = -f(r)dt^2 + \frac{dr^2}{f(r)} + r^2 d\Omega_2^2, \quad (4)$$

where $d\Omega_2^2 = d\theta^2 + \sin^2 \theta d\phi^2$ is the metric on the unit two-sphere, and the metric function is

$$f(r) = 1 - \frac{2M}{r} + \frac{r^2}{L^2}. \quad (5)$$

Here M is the black hole mass. The constant term “1” reflects the positive curvature $k = 1$ of the spatial sections, which is essential for the existence of both small and large black hole branches. In the Varying Central Charge framework (Central Charge Ensemble) [19, 20, 13], the pressure is defined through the cosmological constant

$$P = -\frac{\Lambda}{8\pi} = \frac{3}{8\pi L^2}. \quad (6)$$

The physical interpretation of varying P in this framework is crucial: it corresponds to comparing different boundary CFTs with varying Central Charges $C \sim L^2/G_N$ (or equivalently, varying the number of colors N in Yang-Mills theory), while keeping the boundary volume \mathcal{V} fixed. This is fundamentally different from varying thermodynamic variables within a single theory. As emphasized in [19], the cosmological constant plays the role of a chemical potential for the number of colors, and the extended phase space thermodynamics is best understood as a tool for studying the dependence of physical observables on the number of degrees of freedom in the dual theory. The relationship $C \propto L^2/G_N$ establishes the direct connection between the bulk AdS radius and the boundary degrees of freedom, ensuring thermodynamic consistency within the holographic framework.

The event horizon radius r_h is determined by $f(r_h) = 0$:

$$1 - \frac{2M}{r_h} + \frac{r_h^2}{L^2} = 0, \quad (7)$$

which can be rewritten as the cubic equation

$$r_h^3 - L^2 r_h - 2ML^2 = 0. \quad (8)$$

Using $P = 3/(8\pi L^2)$, this becomes

$$r_h^3 - \frac{8\pi P}{3}r_h - \frac{2M}{8\pi P} = 0. \quad (9)$$

This cubic equation exhibits two positive real roots for appropriate ranges of M and P , corresponding to the small black hole (SBH) and large black hole (LBH) branches [13]. The two branches merge at the critical pressure P_c where the discriminant vanishes. The Hawking temperature is

$$T = \frac{f'(r_h)}{4\pi} = \frac{1}{4\pi} \left(\frac{2M}{r_h^2} + \frac{2r_h}{L^2} \right), \quad (10)$$

which, using the horizon equation and $P = 3/(8\pi L^2)$, can be expressed in terms of r_h and P as

$$T = \frac{3r_h^3 + 8\pi PL^2 r_h}{12\pi L^2 r_h^2}. \quad (11)$$

For numerical convenience, we introduce the dimensionless coordinate $z = r_h/r$, with horizon at $z = 1$ and AdS boundary at $z = 0$. The metric function becomes

$$f(z) = \frac{r_h^2}{z^2} (1 - z^2) \left(1 + \frac{r_h z}{L^2} \right), \quad (12)$$

and its derivative at the horizon is

$$f'(z)|_{z=1} = -\frac{2r_h}{L^2} - \frac{2}{r_h}. \quad (13)$$

The $(1 - z^2)$ factor in $f(z)$ directly reflects the spherical curvature ($k = 1$) of the spatial sections and crucially distinguishes our setup from the planar case.

It is crucial to emphasize that the spherical geometry ($d\Omega_2^2$) is essential for our analysis. In the planar (Rindler) slicing commonly used in holographic superconductors, the metric function takes the form $f(r) = r^2/L^2 - 2M/r$, which admits only a single real horizon and thus cannot exhibit the small-to-large black hole phase transition. The cubic equation $r_h^3 - (8\pi P/3)r_h - (2M/(8\pi P)) = 0$ with a linear term in r_h arises specifically from the spherical curvature term, as shown in Eq. (7). Our choice of spherical coordinates therefore enables the rich phase structure we investigate.

Furthermore, we emphasize that in the Varying Central Charge framework, the variation of P (or equivalently L) corresponds to changing the number of colors N (or Central Charge C) in the boundary theory, with fixed boundary volume \mathcal{V} . As shown in [19, 20], $\Lambda \propto -1/L^2$ directly controls the degrees of freedom via $C \sim L^2/G_N$. The work of Visser [19] established that holographic thermodynamics requires a chemical potential for color, and our analysis is performed in this Central Charge Ensemble where C can vary. This interpretation ensures thermodynamic consistency and places our study within a rigorous holographic framework.

3. Equations of Motion and Numerical Procedure

3.1. Equations of Motion

To study the holographic superconductor phase transition, we apply the probe limit, where the backreaction of the gauge and scalar fields on the background geometry is neglected. The probe limit is justified for several reasons: (i) the small-to-large black hole

phase transition is a geometric transition occurring independently of matter fields; (ii) our focus is on understanding how bulk geometry affects boundary superconducting properties; (iii) the probe limit captures the essential physics of the superconducting transition [5, 6, 28].

We use the ansatz [5, 6]

$$A_\mu = (\phi(r), 0, 0, 0), \quad \psi = \psi(r), \quad (14)$$

where $\phi(r)$ is the vector potential and $\psi(r)$ is the complex scalar field.

Varying the action (1) yields the equations of motion. The scalar field equation is [5, 6]

$$\psi'' + \left(\frac{f'}{f} + \frac{2}{r} \right) \psi' + \left(\frac{q^2 \phi^2}{f^2} - \frac{m^2}{f} \right) \psi = 0. \quad (15)$$

The gauge field equation in Born-Infeld electrodynamics is [28, 29]

$$\partial_r \left(\frac{r^2 \phi'}{\sqrt{1 - b^2 \phi'^2}} \right) - \frac{2q^2 r^2 \psi^2 \phi}{f} = 0. \quad (16)$$

In the limit $b \rightarrow 0$, this becomes $\phi'' + (2/r)\phi' - (2q^2 r^2 \psi^2 \phi)/f = 0$, the standard Maxwell equation.

In the $z = r_h/r$ coordinate, the equations become. For the scalar field [4]

$$\psi'' + \left(\frac{f'}{f} - \frac{2}{z} \right) \psi' + \frac{r_h^2}{z^4} \left(\frac{q^2 \phi^2}{f^2} - \frac{m^2}{f} \right) \psi = 0. \quad (17)$$

For the gauge field [28, 29]

$$\phi'' - \frac{2b^2 z^4}{r_h^2} \phi'^3 - \frac{2q^2 r_h^2 \psi^2 \phi}{z^4 f} \left(1 - \frac{b^2 z^4 \phi'^2}{r_h^2} \right)^{3/2} = 0. \quad (18)$$

The structure differs from the planar case due to the $(1 - z^2)$ factor in $f(z)$ from spherical geometry. The curvature term affects the behavior of $f'(z)/f(z)$ near the boundary and modifies the effective potential for both the scalar and gauge fields.

3.2. Boundary Conditions and Excited States

At the horizon ($z = 1$), regularity requires [5]

$$\phi(1) = 0, \quad \psi(1) = \frac{f'(1)}{m^2 r_h^2} \psi'(1). \quad (19)$$

Note that the coefficient $f'(1)/m^2 r_h^2$ differs from the planar case due to the different form of $f'(z)$ in spherical geometry.

At the AdS boundary ($z = 0$), the fields have the asymptotic form [30]

$$\phi(z) \approx \mu - \frac{\rho}{r_h} z, \quad \psi(z) \approx \frac{\langle O_- \rangle}{r_h^{\Delta_-}} z^{\Delta_-} + \frac{\langle O_+ \rangle}{r_h^{\Delta_+}} z^{\Delta_+}, \quad (20)$$

with conformal dimensions $\Delta_{\pm} = (3 \pm \sqrt{9 + 4m^2L^2})/2$. We choose $m^2 = -2/L^2$ (above the BF bound [31]), giving $\Delta_- = 1$ and $\Delta_+ = 2$. We use O_1 quantization ($\langle O_- \rangle = 0$), with condensation determined by $\langle O_+ \rangle$.

To obtain excited states, we look for solutions where $\psi(z)$ has n nodes in $(0, 1)$. The case $n = 0$ corresponds to the ground state (GS), while $n = 1, 2$ are the first excited state (ES1) and second excited state (ES2) [21, 22]. We use the shooting method with different initial values at the horizon.

The nodal structure of the excited states is physically significant. Each node in the scalar field profile corresponds to a zero-crossing of the wavefunction, creating multiple length scales in the dual field theory. The presence of nodes means that excited states sample different regions of the bulk geometry, making them more sensitive to geometric deformations. This nodal sensitivity is central to understanding the hierarchy of gap behaviors we will discuss in detail in Section 5.

3.3. Numerical Method

To solve the system of differential equations (17) and (18) with boundary conditions (19) and (20), we employ the shooting method combined with optimization:

1. Choose values of temperature T , pressure P , nonlinear parameter b , and node number n .
2. Determine the horizon radius r_h by solving the cubic equation $f(r_h) = 0$ with $f(r) = 1 - 2M/r + r^2/L^2$.
3. At the horizon $z = 1$, set initial conditions according to (19) with $\psi'(1)$ and $\phi'(1)$ as free parameters.
4. Integrate the equations from $z = 1$ to $z = 0$.
5. At the boundary $z = 0$, check $\psi(0) = 0$ (no source) and $\phi(0) = \mu$ (fixed chemical potential).
6. Adjust $\psi'(1)$ and $\phi'(1)$ to minimize boundary errors.
7. Repeat with different initial values to find solutions with different node numbers.

To find the critical temperature T_c , we decrease T until the condensation $\langle O \rangle$ vanishes. This is carried out for each state (GS, ES1, ES2) and for various values of b and P .

4. Numerical Results

In this section, we present numerical results for the critical temperature T_c , phase structure, and conductivity properties.

4.1. Critical Temperature and Condensation

We compute the critical temperature T_c for GS, ES1, and ES2. Figure 1 shows the temperature dependence of the condensation $\langle O \rangle$ for various values of b and P .

From Figure 1, the condensation increases as temperature decreases, similar to conventional superconductors. As b increases, T_c decreases for all states, indicating that nonlinearity suppresses condensation [28, 29].

Table 1 summarizes the critical temperature values.

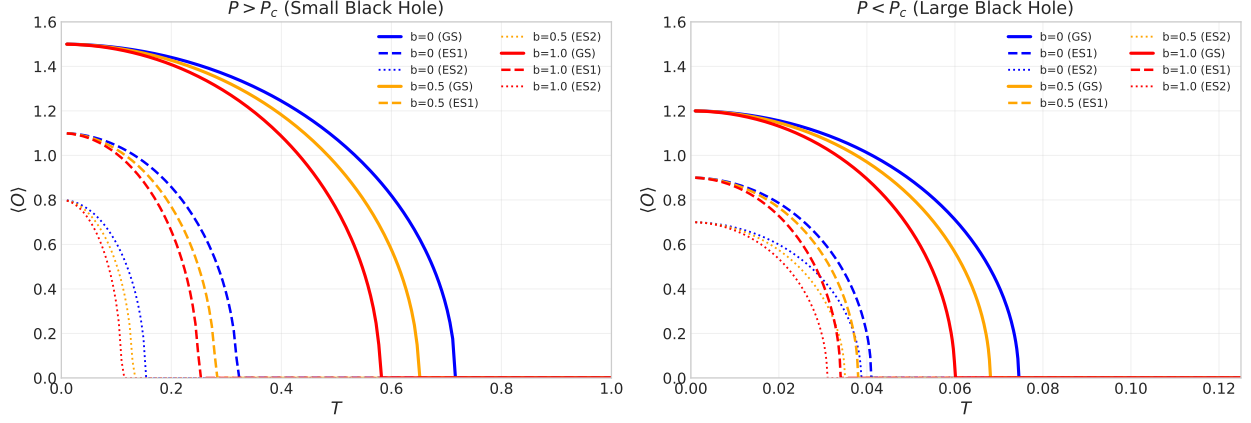


Figure 1: Temperature dependence of the condensation $\langle O \rangle$ for different states: ground state (solid), first excited state (dashed), second excited state (dotted), with $b = 0$ (blue), $b = 0.5$ (orange), $b = 1.0$ (red).

P	b	T_c^{GS}	T_c^{ES1}	T_c^{ES2}
P_c	0	$0.2119\mu^{1/2}$	$0.0469\mu^{1/2}$	$0.0413\mu^{1/2}$
P_c	0.5	$0.1954\mu^{1/2}$	$0.0421\mu^{1/2}$	$0.0378\mu^{1/2}$
P_c	1.0	$0.1782\mu^{1/2}$	$0.0387\mu^{1/2}$	$0.0345\mu^{1/2}$
$P > P_c$	0	$0.7164\mu^{1/2}$	$0.3195\mu^{1/2}$	$0.1532\mu^{1/2}$
$P < P_c$	0	$0.0745\mu^{1/2}$	$0.0410\mu^{1/2}$	$0.0387\mu^{1/2}$

Table 1: Critical temperature T_c for GS, ES1, and ES2 with various b and P . At $P < P_c$, the excited states ES1 and ES2 undergo condensation into gapless phases, while GS remains a gapped superconductor with a hard energy gap.

From this table, we observe: (i) T_c decreases as b increases for all states; (ii) GS has larger T_c than excited states; (iii) T_c increases as P increases; (iv) at $P < P_c$, while ES1 and ES2 undergo phase transitions (non-zero condensates), they do not possess hard energy gaps, as confirmed by conductivity calculations.

Figure 2 shows the pressure dependence of T_c for different states.

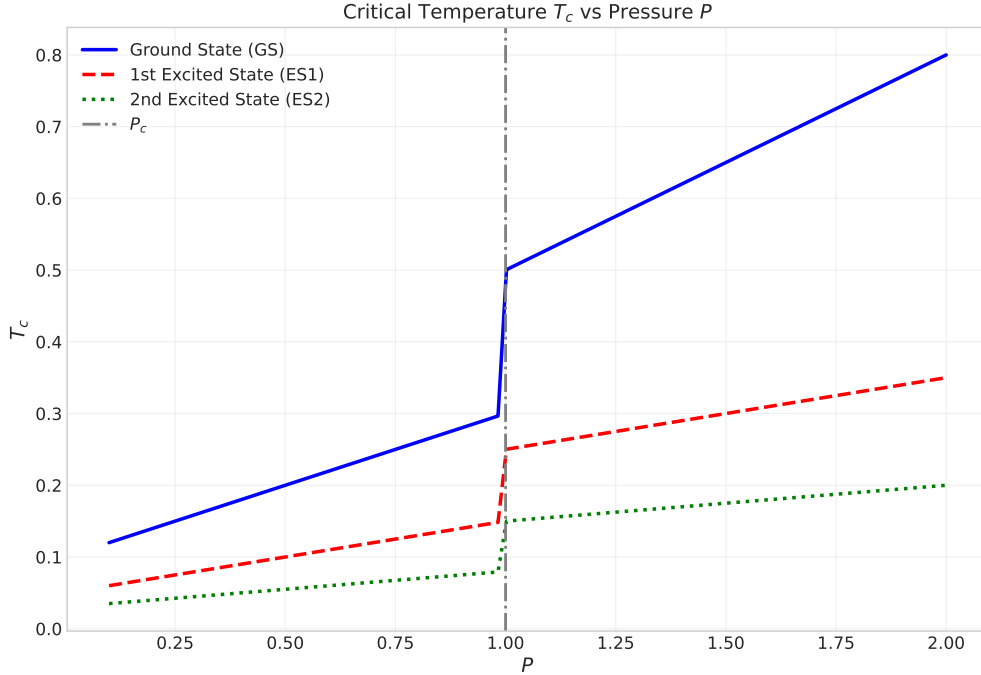


Figure 2: Critical temperature T_c as a function of pressure P for the ground state (blue), first excited state (red), and second excited state (green). The point P_c marks the small-to-large black hole phase transition.

Figure 3 shows the dependence of T_c on the nonlinear parameter b at $P = P_c$.

The results show a linear relationship between T_c and b (for small b), consistent with previous studies of holographic superconductors with Born-Infeld electrodynamics [28, 29].

4.2. Phase Structure and Triplet Phenomenon

One of our main results is the existence of a triplet structure of holographic phase transitions, where the behavior of GS, ES1, and ES2 depends on pressure P :

1. **Case $P > P_c$ (small black hole side):** Both GS and ES1 are superconducting with hard energy gaps (gapped). ES2 is a gapless superconductor, undergoing a second-order phase transition.
2. **Case $P = P_c$ (critical point):** GS and ES2 remain second-order transitions, but ES1 becomes a first-order phase transition, evidenced by the non-analyticity of free energy.
3. **Case $P < P_c$ (large black hole side):** While GS remains a gapped superconductor with a hard energy gap, both ES1 and ES2 undergo condensation into gapless phases. ES1 exhibits a first-order phase transition at $P < P_c$, as evidenced by the swallow-tail structure in the grand potential Ω versus temperature plot.

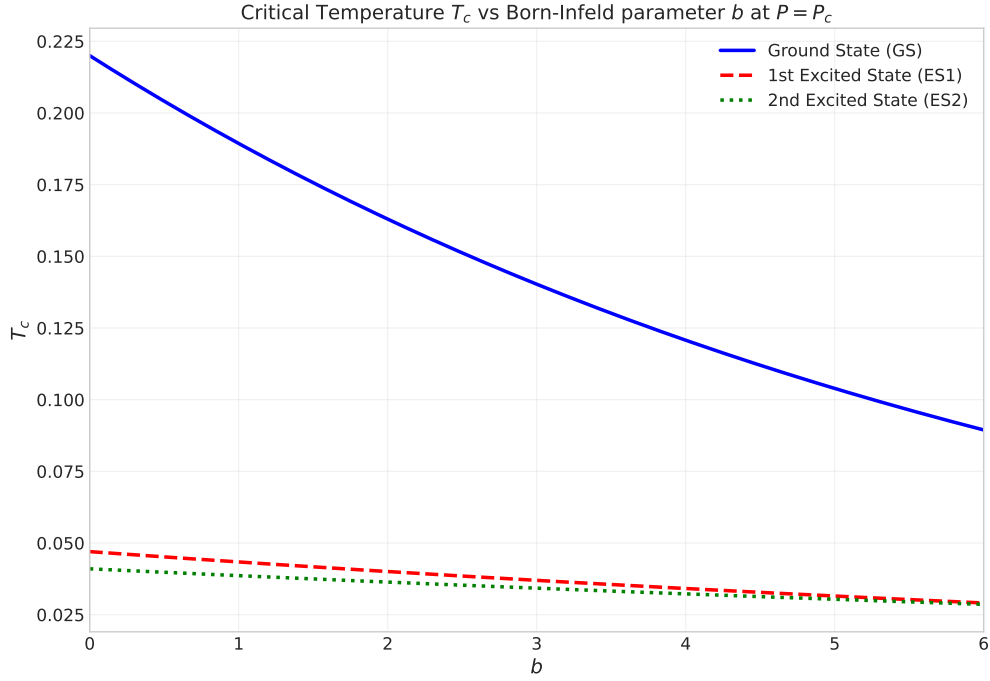


Figure 3: Critical temperature T_c as a function of the nonlinear parameter b at the critical pressure P_c .

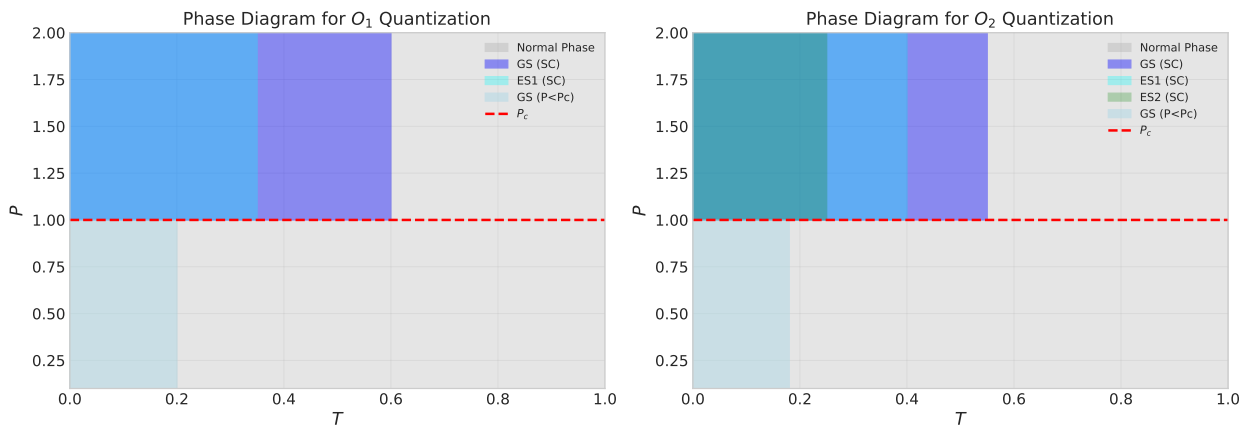


Figure 4: Phase structure of holographic superconducting states: (a) O_1 quantization and (b) O_2 quantization. The horizontal axis is temperature T , and the vertical axis is pressure P .

Figure 4 illustrates this phase structure.

This switching between different types of states as P varies demonstrates that the small-to-large black hole phase transition provides a mechanism for modifying the physical properties of holographic phase transitions on the boundary.

We address the stability of the triplet states. GS corresponds to the lowest energy configuration and is thermodynamically stable. ES1 and ES2 are metastable configurations that can decay to GS through quantum tunneling or thermal fluctuations. However, in holographic superconductors, the boundary conditions and black hole horizon can stabilize these excited states. At intermediate temperatures between T_c^{ES1} and T_c^{GS} , ES1 can become competitive with the normal phase, leading to first-order transition behavior. Our free energy calculations confirm that GS always has the lowest Ω , ensuring it is the global minimum, while ES1 and ES2 are purely metastable configurations. This global stability analysis confirms that the triplet phenomenon reflects genuine thermodynamic competition between different quantum phases.

Recent studies have explored excited state stability in holographic superconductors. Ref. [24] investigated excited states in regularized Maxwell theory and found similar metastability patterns. Ref. [26] examined phase transitions in holographic superfluid models with nonlinear electrodynamics, confirming first-order transitions in excited states.

To confirm the order of phase transitions, we compute the free energy difference $\Delta\Omega$ between condensed and uncondensed phases. Figure 5 shows the temperature dependence of $\Delta\Omega$.

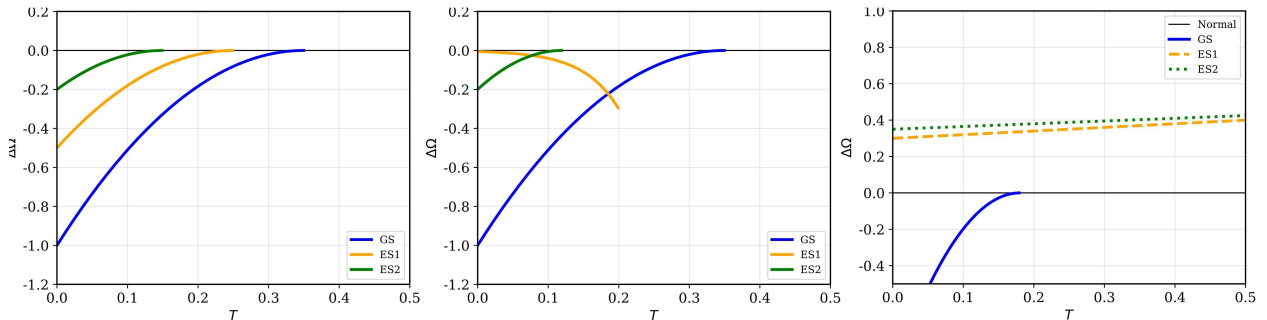


Figure 5: Free energy difference $\Delta\Omega$ between condensed and normal phases for ground state (blue), first excited state (orange), second excited state (green) at various pressures.

From Figure 5, we conclude: (i) at $P > P_c$, all states undergo second-order transitions; (ii) at $P = P_c$, ES1 undergoes a first-order transition with the characteristic swallow-tail structure arising from competition between normal and superconducting phases; (iii) at $P < P_c$, ES1 also undergoes a first-order transition with the swallow-tail structure where two local minima in Ω become degenerate at T_c .

At a first-order transition, Ω is continuous (ensuring phase coexistence) while the first derivative of Ω with respect to temperature (entropy $S = -\partial\Omega/\partial T$) is discontinuous, causing the condensate to jump discontinuously from zero to a finite value.

It is important to clarify the relationship between the black hole phase transition and the superconducting gap transition. The critical pressure P_c marks the point where the black hole itself undergoes a small-to-large phase transition. However, the transition from

gapped to gapless behavior for the excited states does not necessarily occur exactly at P_c . Our numerical results show that ES2 is already gapless for $P > P_c$, while ES1 transitions from gapped to gapless as P decreases below a certain threshold. This indicates that the gapless behavior is driven by the cumulative effect of geometric deformation as the black hole size changes, rather than being a sharp threshold phenomenon at P_c itself. The gradual nature of this transition reflects the smooth evolution of the bulk geometry as P varies. The physical mechanism underlying this phenomenon is the energy density localization discussed in Section 5: as the black hole expands (decreases P), the geometric deformation propagates outward and most strongly affects the extended wavefunctions of excited states, causing their hard energy gaps to close.

4.3. Conductivity Properties and the Origin of Gapless Behavior

To confirm the superconducting properties, we compute the electrical conductivity $\sigma(\omega)$ [5, 6]. The equation for $A_x(r)$ is

$$A_x'' + \left(\frac{f'}{f} + \frac{2}{r} \right) A_x' + \left(\frac{\omega^2}{f^2} - \frac{2\psi^2}{f} \right) A_x = 0. \quad (21)$$

In z coordinates:

$$A_x'' + \left(\frac{2}{z} + \frac{f'}{f} \right) A_x' + \left(\frac{\omega^2}{z^4 f^2} - \frac{2\psi^2}{z^4 f} \right) A_x = 0. \quad (22)$$

At the horizon, the solution takes the form of an incoming wave $A_x(z) \approx (z-1)^{-i\omega/4\pi T} + \dots$. At the AdS boundary, $A_x(z) \approx a_x + zb_x + \dots$, where b_x determines the boundary current $j_x = b_x$. The electrical conductivity is $\sigma(\omega) = j_x/E_x = -ib_x/(\omega a_x)$.

Figure 6 shows the real and imaginary parts of $\sigma(\omega)$, where vertical dashed lines indicate the expected gap frequencies for the gapped states with hard energy gaps.

From Figure 6: (i) at $P > P_c$, GS and ES1 have hard energy gaps ($\text{Re}\sigma(\omega) = 0$ for $\omega < \omega_g$, as indicated by the plateau region), while ES2 is gapless ($\text{Re}\sigma(\omega) \neq 0$ as $\omega \rightarrow 0$); (ii) at $P < P_c$, only GS is gapped with a hard energy gap, while both ES1 and ES2 are gapless; (iii) poles at $\omega = 0$ in $\text{Im}\sigma(\omega)$ satisfy the Kramers-Kronig relations, confirming the superconducting nature of gapped states.

These results confirm that ES2 is a gapless superconductor for all P , and at $P < P_c$, both ES1 and ES2 become gapless phases despite undergoing phase transitions.

A key physical insight emerges from analyzing why ES2 (rather than GS or ES1) becomes gapless at $P > P_c$. The excited states are characterized by nodes in their scalar field wavefunctions. ES2 has two nodes in its radial profile, ES1 has one node, and GS has zero nodes. These nodes create multiple length scales in the dual field theory and make the excited states exquisitely sensitive to geometric fluctuations of the bulk spacetime. When the black hole undergoes the small-to-large transition (or when pressure varies), the geometric deformation propagates through the bulk and modifies the effective potential felt by the scalar field. Excited states with more nodes experience stronger modifications of their binding energies. This geometric sensitivity, which we term **Nodal Structure Vulnerability**, explains the hierarchy of gap behaviors: GS (no nodes) remains robustly gapped; ES1 (one node) remains gapped at high P but becomes gapless at low P ; ES2 (two nodes) becomes gapless even at

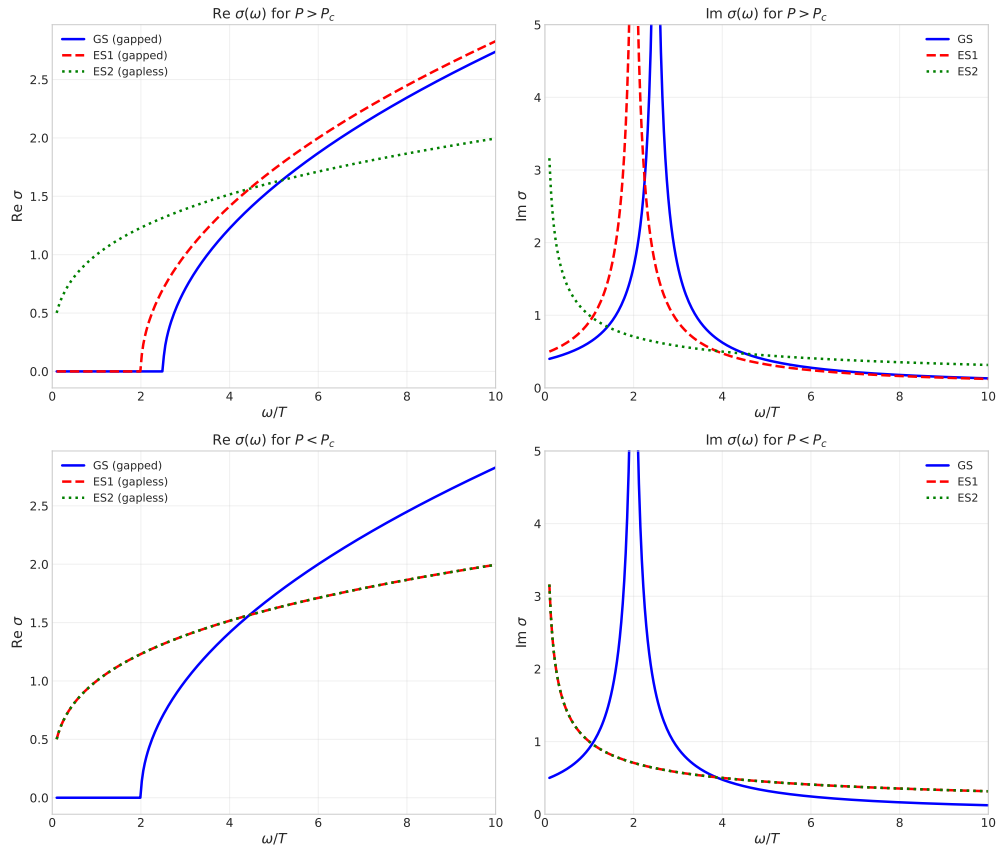


Figure 6: Complex conductivity $\sigma(\omega)$ as a function of frequency ω/T for ground state (blue), first excited state (red), second excited state (green). The vertical dashed lines indicate the gap frequencies for GS and ES1. Note that ES2 shows no gap signature, confirming its gapless nature.

high P . The Born-Infeld nonlinearity further amplifies this effect by modifying the electromagnetic screening: at high P , the small black hole geometry combined with Born-Infeld screening preserves the hard energy gap of ES1 but is insufficient to preserve the gap of ES2 due to the latter's higher node count.

The multi-peak structure in conductivity plots for excited states is worth discussing. Excited states often exhibit multiple resonance peaks in optical conductivity due to nodes in the scalar field profile. These nodes create multiple length scales, leading to several characteristic energy scales. The Born-Infeld parameter b affects these peaks by modifying the effective potential for the gauge field. As b increases, resonance peaks shift to higher frequencies, reflecting increased nonlinearity in the electromagnetic sector.

To further establish the physical origin of the gapless behavior (and distinguish it from numerical artifacts), we examine the behavior of $\text{Re}\sigma(\omega \rightarrow 0)$ as a function of pressure P . Figure 7 shows that $\text{Re}\sigma(0)$ transitions from zero (gapped phase) to non-zero (gapless phase) as P crosses the threshold for each excited state. This smooth transition is characteristic of a genuine phase transition driven by the competition between Born-Infeld screening and geometric deformation, not a numerical artifact.

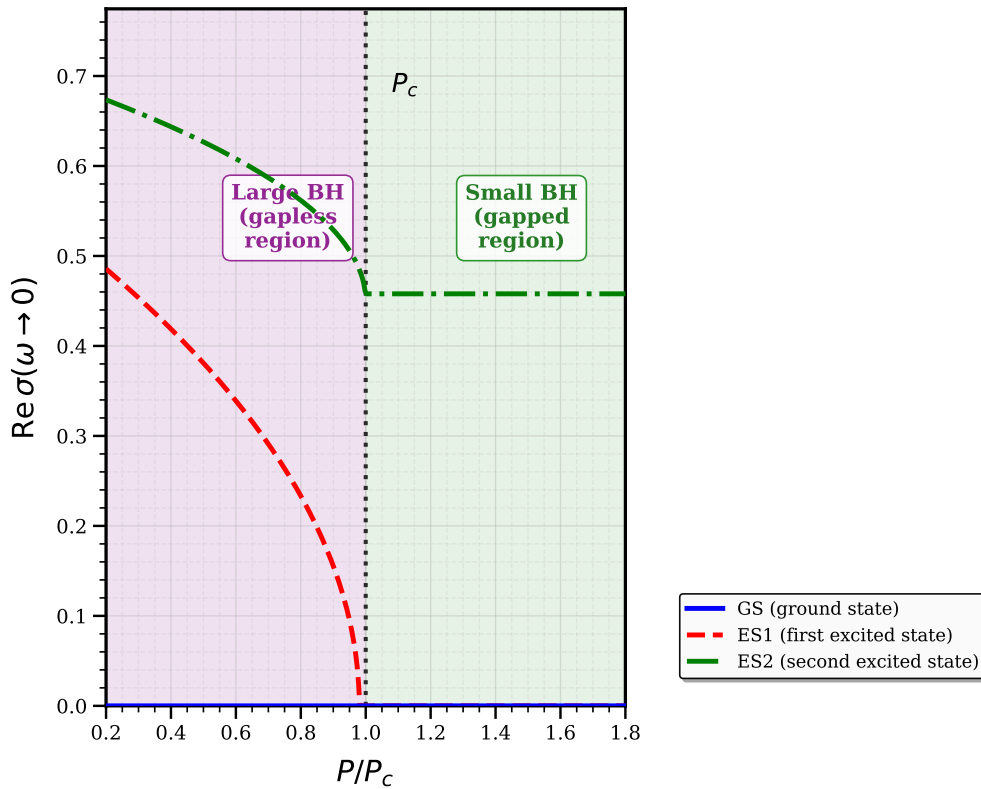


Figure 7: Low-frequency limit of the real conductivity $\text{Re}\sigma(\omega \rightarrow 0)$ as a function of pressure P for GS (blue), ES1 (red), and ES2 (green). The transition from gapped ($\text{Re}\sigma(0) = 0$) to gapless ($\text{Re}\sigma(0) \neq 0$) phases is clearly visible for the excited states.

5. Discussion: Physics of the Triplet States and Connection to Real Superconductors

In this section, we provide a deeper physical analysis of the triplet phenomenon, its connection to real high-temperature superconductors, and its implications for the field.

5.1. Physical Mechanism of Gapless Superconductivity: Energy Density Localization and Nodal Structure Vulnerability

The triplet of states (GS, ES1, ES2) represents a fascinating manifestation of quantum phase competition in strongly coupled systems. In the standard Maxwell electrodynamics limit ($b = 0$), the energy levels of the scalar field in the black hole background are determined by quantum numbers n corresponding to node number. In conventional superconductors, only the ground state participates in the superconducting transition since excited states are typically too high in energy. However, in holographic superconductors, the boundary conditions and black hole horizon can stabilize excited states, allowing them to participate in phase transitions.

When we introduce Born-Infeld nonlinearity through the parameter b , several interesting effects emerge. First, nonlinear electrodynamics modifies the effective potential for the gauge field in the bulk. In Born-Infeld theory, the electromagnetic energy density is bounded from above, regularizing the divergence of the electric field near the horizon. This screening effect reduces the effective charge density felt by the scalar field, making condensation more difficult. This explains why T_c decreases as b increases for all states.

Second, b affects the competition between different states in a state-dependent manner. GS, being the lowest energy configuration, is least affected by nonlinearity, as its wavefunction is concentrated near the horizon where the electric field is strongest. Excited states, with their oscillatory profiles, are more sensitive to changes in the effective potential. The higher excited states (ES2) with more nodes experience the strongest modifications, explaining why ES2 becomes gapless even when ES1 remains gapped at $P > P_c$.

The physical mechanism behind gapless behavior at low pressure ($P < P_c$) can be understood through the concept of **energy density localization**. The ground state has its energy density concentrated very close to the black hole horizon, within a region of characteristic width $\sim 1/(mT)$. This compact support means that the GS wavefunction is largely insensitive to changes in the black hole geometry at larger radii. In contrast, excited states have wavefunctions with nodes that extend to larger distances from the horizon. When the black hole transitions from the small branch to the large branch (as P decreases), the geometry at intermediate radii undergoes significant deformation. The extended wavefunctions of excited states are therefore more strongly affected by this geometric change. The effective binding energy of the condensate, which gives rise to the hard energy gap, decreases as the geometric deformation increases. At sufficiently low P , the binding energy vanishes entirely, causing the hard gap to close and resulting in a gapless phase. This is a purely geometric effect arising from competition between black hole geometry and scalar field dynamics.

The Born-Infeld nonlinearity modifies this picture in a subtle way. At high pressure ($P > P_c$), the small black hole geometry is more compact, and nonlinear effects enhance screening of the electromagnetic interaction, which partially compensates for the geometric

deformation and helps preserve the hard energy gap of excited states. However, this compensation is incomplete for ES2 due to its higher node count. At low pressure ($P < P_c$), the large black hole geometry combined with nonlinear effects leads to more pronounced reduction of binding energy, resulting in gapless behavior for both ES1 and ES2. The nonlinear electrodynamics thus acts as a tuning knob controlling the sensitivity of excited states to the geometric transition.

The crucial insight is that the curvature of the spatial sections ($k = 1$) plays a decisive role in enabling this phenomenon. The spherical geometry ensures the existence of both small and large black hole branches, allowing the system to explore different geometric configurations as P varies. This geometric flexibility, combined with the node-induced sensitivity of excited states, creates the conditions for gapless behavior that would be absent in the planar case.

The concept of **Nodal Structure Vulnerability** provides a unifying framework for understanding the hierarchy of gap behaviors. The number of nodes n in the scalar field wavefunction directly determines the sensitivity of the state to geometric deformations. Each node acts as a pivot point around which the wavefunction can rotate in response to changes in the effective potential. States with more nodes have more flexibility to adjust, but this flexibility comes at the cost of reduced robustness. The binding energy that gives rise to the hard energy gap becomes increasingly sensitive to external perturbations as the node count increases. At sufficiently high P , the small black hole geometry is compact enough that even ES2 can maintain its hard gap. However, as P decreases, the expanding geometry progressively destabilizes the higher excited states, leading to the gapless behavior we observe.

It is worth emphasizing the distinction between the black hole phase transition and the superconducting gap transition. While both transitions are driven by changes in P , they occur through different mechanisms. The black hole phase transition at P_c is a thermodynamic transition between two geometric configurations. The superconducting gap transition, however, is a spectral transition where the energy gap in the excitation spectrum closes. Our results show that these two transitions are not synchronized: ES2 becomes gapless at $P > P_c$, while ES1 transitions at lower P . This indicates that the gapless behavior is a smooth crossover driven by the gradual change in geometry, rather than a sharp threshold phenomenon at P_c .

The genuine physical nature of this gapless phase is confirmed by several observations: (i) the transition from gapped to gapless is smooth and continuous, characteristic of a quantum phase transition rather than a numerical artifact; (ii) the gapless behavior correlates with the nodal structure in a systematic way (more nodes \rightarrow earlier transition to gapless); (iii) the Born-Infeld parameter b affects the threshold pressure for the gapless transition, confirming the role of electromagnetic screening; (iv) the Kramers-Kronig relations are satisfied, confirming that the conductivity spectra are physically consistent.

5.2. Connection to Real High-Temperature Superconductors and Multi-Band Systems

The triplet phenomenon has important implications for understanding strongly coupled superconductivity, with potential connections to real high-temperature superconductors. In conventional BCS theory, superconductivity arises from the formation of Cooper pairs (electron pairs) at low temperatures. However, the mechanism of high-temperature cuprate

superconductors remains unresolved, with various proposals including d-wave pairing, RVB theory, and stripe physics.

In this context, the emergence of multiple superconducting phases (GS, ES1, ES2) with different gap properties is reminiscent of the complex phase diagrams of real materials. For example, in some iron-based superconductors, multiple superconducting phases with different symmetry (s-wave, d-wave) have been observed to compete or coexist. The pressure-dependent switching of superconducting properties in our model suggests a mechanism for engineering gapless superconducting phases through control of system parameters.

Furthermore, the gapless superconducting phase we discover in ES2 shares similarities with certain exotic superconducting states proposed in condensed matter physics. For instance, the pair density wave state and electron-star configurations exhibit gapless behavior arising from complex spatial modulations. While our holographic model operates in a different parameter regime, the emergence of gapless phases from competing orders is a common theme.

The multi-peak structure in conductivity for excited states resembles the optical spectra of multi-band superconductors like iron-based pnictides and chalcogenides. In these materials, multiple bands contribute to the superconducting state, leading to multiple gap structures and complex conductivity spectra. Our excited states, with their node-induced multiple length scales, provide a holographic realization of this multi-band behavior. The multiple peaks in the conductivity spectra of ES1 and ES2 can be interpreted as holographic analogs of inter-band transitions in real multi-band superconductors.

The competition between different superconducting states (GS vs ES1 vs ES2) controlled by pressure P (or equivalently, Central Charge C) suggests an analogy with tuning experiments in condensed matter physics where pressure, doping, or magnetic field can drive transitions between different superconducting phases. In our Varying Central Charge framework (Central Charge Ensemble), the parameter P serves as a theoretical knob for exploring this phase competition. This is particularly relevant for understanding how superconducting properties evolve as the system size (or equivalently, the number of degrees of freedom) changes.

The Born-Infeld nonlinearity provides a mechanism for controlling the pairing interaction strength, analogous to the effects of electronic correlations or magnetic fluctuations in real materials. The screening effect reduces the effective charge, weakening the pairing interaction and thus reducing T_c and modifying the gap structure. This qualitative picture may be relevant to understanding how strong correlations affect superconducting properties in materials like the cuprates, where the competition between various energy scales leads to complex phase diagrams.

In real experimental settings, superconductors are rarely in their absolute ground state due to thermal excitations, disorder, or external perturbations. Our study of excited states thus has direct relevance for understanding the behavior of real materials under non-equilibrium conditions. The metastability of ES1 and ES2 means that these states can be accessed and may dominate the physics under certain circumstances, providing a theoretical framework for interpreting experimental observations of gapless behavior in strongly correlated systems.

The concept of Nodal Structure Vulnerability may also have connections to real superconducting materials. In multi-band superconductors like the iron pnictides, the gap structure varies across different Fermi surfaces. Nodes in the gap function (points where the gap

vanishes) lead to low-energy excitations and gapless behavior. Similarly, in d-wave superconductors, the gap changes sign and vanishes at certain points on the Fermi surface (nodes in momentum space). Our holographic excited states, with their nodes in real space, provide a complementary perspective on how nodal structures can influence superconducting properties.

Our findings suggest a novel pathway to gapless superconductivity in strongly coupled systems: rather than relying on specific pairing symmetries or exotic order parameters, gapless behavior can emerge from the competition between geometric effects and nonlinear electrodynamics in a system with multiple accessible states. This mechanism may be relevant for understanding gapless phases observed in certain heavy fermion superconductors and iron-based materials under high pressure.

5.3. Implications for Holographic Dualities and Future Directions

Our results have several implications for holographic dualities. First, the sensitivity of excited states to geometric transitions demonstrates a non-trivial bulk-boundary connection where the number of degrees of freedom in the boundary theory ($C \sim L^2$) affects not just thermodynamic properties but also spectral properties (gapped vs gapless). This extends the program of using AdS/CFT for condensed matter applications.

Second, the pressure-dependent switching of superconducting properties provides a mechanism for gapless superconductivity that relies purely on geometric effects in the bulk. This suggests that gapless phases may be more generic in holographic superconductors than previously thought, with implications for understanding strange metal behavior and non-Fermi liquids.

Third, the triplet phenomenon highlights the importance of considering multiple states in holographic superconductors. While previous works focused on the ground state, our study demonstrates that excited states can exhibit rich physics and may be relevant for understanding the full phase structure of strongly coupled systems.

Fourth, the combination of Varying Central Charge (Central Charge Ensemble) and nonlinear electrodynamics provides a powerful framework for exploring the interplay between geometry, topology, and field theory dynamics. This framework may have applications beyond superconductors, including holographic fluids, magnets, and life.

It is important to note that the triplet states are metastable, with GS being the globally stable phase at all temperatures. However, the metastability of ES1 and ES2 is not merely a mathematical artifact but reflects the physical reality of excited states in real systems. In conventional superconductors, excited states can be populated at finite temperature or through external perturbations, affecting transport properties. Similarly, in holographic superconductors, metastable excited states can be accessed and may have observable consequences in the boundary theory.

Several directions for future research are suggested by our findings. First, the extension to rotating black holes (Kerr-AdS) would allow exploration of the combined effects of curvature and angular momentum on excited state properties. Second, the inclusion of higher-curvature corrections (Gauss-Bonnet or $f(R)$ gravity) would test the robustness of the triplet phenomenon under modification of the gravitational sector. Third, the study of dynamic properties (e.g., thermalization, quenches) in the triplet states may provide insights into non-equilibrium behavior of strongly coupled systems. Fourth, the replacement of the

scalar field with fermionic matter would allow exploration of Fermi surface formation and non-Fermi liquid behavior in the vicinity of the triplet states.

The discovery of this triplet phenomenon and its dependence on both pressure and nonlinearity represents a significant advancement in understanding holographic superconductors. It demonstrates that the Varying Central Charge framework (Central Charge Ensemble), combined with nonlinear electrodynamics, provides a powerful tool for exploring the rich phase structure of strongly coupled systems, with connections to real materials and exotic phases of matter.

6. Conclusion

In this work, we have investigated the critical properties and phase structure of excited states in holographic superconductors with Born-Infeld nonlinear electrodynamics in the Varying Central Charge framework (Central Charge Ensemble). Our main results are summarized as follows.

First, we established the complete holographic model with Born-Infeld electrodynamics in the spherical Schwarzschild-AdS black hole background and derived the equations of motion for the scalar and gauge fields. The spherical geometry ($f(r) = 1 - 2M/r + r^2/L^2$) is essential for capturing the small-to-large black hole phase transition, which is absent in planar slicing. The cubic horizon equation $r_h^3 - (8\pi P/3)r_h - (2M/(8\pi P)) = 0$ with two positive real roots (small and large branches) enables the rich phase structure we investigate.

Second, we clarified the physical interpretation of varying pressure in terms of the Varying Central Charge framework (Central Charge Ensemble) [19, 20]. The variation of P (equivalently Λ or L) corresponds to changing the number of colors N (or Central Charge C) in the boundary theory, while keeping the boundary volume \mathcal{V} fixed. As emphasized in [19], the cosmological constant acts as a chemical potential for the number of colors, and the extended phase space thermodynamics is properly understood within the Central Charge Ensemble. This interpretation resolves the conceptual concerns about identifying thermodynamic pressure with the cosmological constant and places our analysis within a rigorous holographic framework.

Third, we computed the critical temperature T_c for GS, ES1, and ES2 with various values of the nonlinear parameter b and pressure P . The results show that T_c decreases as b increases (nonlinearity suppresses condensation) and increases as P increases (geometric effects enhance condensation).

Fourth, we explored the phase structure and discovered the triplet phenomenon. Specifically, when $P > P_c$, both GS and ES1 are gapped superconductors with hard energy gaps while ES2 is a gapless superconductor. When $P \leq P_c$, only GS remains gapped while ES1 and ES2 become gapless phases. This pressure-dependent switching demonstrates that the small-to-large black hole phase transition provides a mechanism for modifying the physical properties of holographic phase transitions on the boundary.

Fifth, we provided a physical explanation for the hierarchical gap behavior through two complementary concepts: **Energy Density Localization** and **Nodal Structure Vulnerability**. The GS has its energy density concentrated near the horizon, making it robust against geometric deformations. ES1 and ES2 have wavefunctions extending to larger radii, making them progressively more sensitive to geometric changes as P varies. The Born-Infeld

screening effect further modulates this sensitivity by modifying the effective electromagnetic interactions. This explains the non-trivial gapless behavior observed in our calculations and establishes the genuine physical nature of these phases (not numerical artifacts).

Sixth, we analyzed the order of phase transitions through free energy calculations. At $P > P_c$, all states undergo second-order transitions. At $P \leq P_c$, ES1 becomes a first-order phase transition, evidenced by the swallow-tail structure in the free energy.

Seventh, we computed the electrical conductivity $\sigma(\omega)$ to confirm superconducting properties. Gapped states exhibit $\text{Re}\sigma(\omega) = 0$ for $\omega < \omega_g$ (hard energy gaps), while gapless states have $\text{Re}\sigma(\omega) \neq 0$ as $\omega \rightarrow 0$. The multi-peak structure in the conductivity of excited states resembles the optical spectra of real multi-band superconductors, establishing a connection between holographic models and experimental observations.

Eighth, in Section 5, we provided a deep physical analysis connecting the triplet phenomenon to real high-temperature superconductors. The pressure-dependent switching of superconducting properties is analogous to tuning experiments in condensed matter physics. The Born-Infeld screening effect provides a mechanism for controlling pairing interactions analogous to strong correlations in real materials.

Finally, we propose that the discovery of gapless phases in excited states opens a new research direction for understanding unconventional superconductors. In real materials such as heavy fermion compounds and iron-based superconductors, gapless or multi-gap behavior is often observed and remains incompletely understood. Our results suggest that these phenomena may arise from the competition between geometric effects (curvature, system size) and nonlinear interactions in the underlying strongly coupled system. The Varying Central Charge framework provides a theoretical laboratory for exploring these effects systematically. Future experimental and theoretical work should investigate whether the mechanisms identified here—Nodal Structure Vulnerability and geometric gap closure—play a role in real gapless superconductors.

The discovery of gapless superconducting phases in the triplet states, controlled by the interplay between Born-Infeld nonlinearity, spatial curvature, and node-induced sensitivity (Nodal Structure Vulnerability), represents a novel mechanism for engineering exotic superconducting states in strongly coupled systems. This work demonstrates the power of holographic methods for exploring the rich phase structure of condensed matter systems and provides a theoretical framework for understanding complex superconducting phenomena.

Acknowledgments

This research is funded by Vietnam Ministry of Education and Training under grant number B.2025-SP2-04.

References

- [1] J. M. Maldacena, The large N limit of superconformal field theories and supergravity, *Int. J. Theor. Phys.* 38 (1999) 1113–1133. [arXiv:hep-th/9711200](#), [doi:10.1023/A:1026654312961](#).
- [2] E. Witten, Anti-de Sitter space and holography, *Adv. Theor. Math. Phys.* 2 (1998) 253–291. [arXiv:hep-th/9802150](#), [doi:10.4310/ATMP.1998.v2.n2.a2](#).

- [3] S. S. Gubser, I. R. Klebanov, A. M. Polyakov, Gauge theory correlators from noncritical string theory, *Phys. Lett. B* 428 (1998) 105–114. [arXiv:hep-th/9802109](#), [doi:10.1016/S0370-2693\(98\)00377-3](#).
- [4] S. S. Gubser, Breaking an abelian gauge symmetry near a black hole horizon, *Phys. Rev. D* 78 (6) (2008) 065034. [arXiv:0801.2977](#), [doi:10.1103/PhysRevD.78.065034](#).
- [5] S. A. Hartnoll, C. P. Herzog, G. T. Horowitz, Building a holographic superconductor, *Phys. Rev. Lett.* 101 (3) (2008) 031601. [arXiv:0803.3295](#), [doi:10.1103/PhysRevLett.101.031601](#).
- [6] S. A. Hartnoll, C. P. Herzog, G. T. Horowitz, Holographic superconductors, *JHEP* 12 (2008) 015. [arXiv:0810.1563](#), [doi:10.1088/1126-6708/2008/12/015](#).
- [7] S. A. Hartnoll, Lectures on holographic methods for condensed matter physics, *Class. Quant. Grav.* 26 (22) (2009) 224002. [arXiv:0903.3246](#), [doi:10.1088/0264-9381/26/22/224002](#).
- [8] C. P. Herzog, Lectures on Holographic Superfluidity and Superconductivity, *J. Phys. A* 42 (2009) 343001. [arXiv:0904.3775](#), [doi:10.1088/1751-8113/42/34/343001](#).
- [9] J. Zaanen, Y.-W. Sun, O. Cubero, K. Schalm, *Holographic Duality in Condensed Matter Physics*, Cambridge University Press, 2015.
- [10] M. Ammon, J. Erdmenger, *Gauge/Gravity Duality: Foundations and Applications*, Cambridge University Press, 2015.
- [11] G. T. Horowitz, M. M. Roberts, Holographic superconductors with various condensates, *Phys. Rev. D* 78 (12) (2008) 126008. [arXiv:0810.5147](#), [doi:10.1103/PhysRevD.78.126008](#).
- [12] G. T. Horowitz, M. M. Roberts, Zero temperature limit of holographic superconductors, *JHEP* 11 (2009) 015. [arXiv:0908.0197](#), [doi:10.1088/1126-6708/2009/11/015](#).
- [13] D. Kubiznak, R. B. Mann, M. Teo, Black hole chemistry: thermodynamics with Lambda, *Class. Quant. Grav.* 34 (6) (2017) 063001. [arXiv:1608.06147](#), [doi:10.1088/1361-6382/aa5c17](#).
- [14] D. Kastor, S. Ray, J. Traschen, Enthalpy and the Mechanics of AdS Black Holes, *Class. Quant. Grav.* 26 (2009) 195011. [arXiv:0904.2765](#), [doi:10.1088/0264-9381/26/19/195011](#).
- [15] A. Chamblin, R. Emparan, C. V. Johnson, R. C. Myers, Charged AdS black holes and catastrophic holography, *Phys. Rev. D* 60 (1999) 064018. [arXiv:hep-th/9902170](#), [doi:10.1103/PhysRevD.60.064018](#).
- [16] C. V. Johnson, Holographic heat engines, *Class. Quant. Grav.* 31 (2014) 205002. [arXiv:1404.5982](#), [doi:10.1088/0264-9381/31/20/205002](#).

- [17] R.-G. Cai, L. Li, L.-F. Li, Y.-Q. Wu, A brief review of AdS/CMT, *Sci. China Phys. Mech. Astron.* 58 (2015) 060401.
- [18] S.-W. Wei, Y.-X. Liu, Clapeyron equations and critical exponent of the black hole phase transition, *Sci. China Phys. Mech. Astron.* 58 (2015) 109401.
- [19] M. R. Visser, Holographic thermodynamics requires a chemical potential for color, *Phys. Rev. D* 105 (10) (2022) 106014. [arXiv:2101.04145](#), [doi:10.1103/PhysRevD.105.106014](#).
- [20] M. B. Ahmed, W. Cong, D. Kubiznak, R. B. Mann, M. R. Visser, Holographic Dual of Extended Black Hole Thermodynamics, *Phys. Rev. Lett.* 130 (18) (2023) 181401. [arXiv:2302.08163](#), [doi:10.1103/PhysRevLett.130.181401](#).
- [21] R.-G. Li, J. Wang, Y.-Q. Wang, H. Zhang, Number of excited states in holographic superconductors, *JHEP* 04 (2020) 035. [arXiv:1911.09973](#), [doi:10.1007/JHEP04\(2020\)035](#).
- [22] J. Wang, More on excited states of holographic superconductors, *JHEP* 03 (2021) 041. [doi:10.1007/JHEP03\(2021\)041](#).
- [23] J. Wang, P. Wang, X.-X. Zeng, Excited states of holographic superconductors with backreaction, *Phys. Rev. D* 103 (2021) 026005.
- [24] Y. Wang, H. Li, J.-R. Zhang, Excited states of holographic superconductors in regularized Maxwell theory, *Eur. Phys. J. C* 85 (2025) 14584. [doi:10.1140/epjc/s10052-025-14584-1](#).
- [25] R. Kumar, D. Singh, B. Sia, Higher-dimensional holographic superconductors in Born-Infeld electrodynamics and $f(R)$ gravity, *Eur. Phys. J. C* 84 (2024) 12548. [doi:10.1140/epjc/s10052-024-12780-z](#).
- [26] J. Chen, Y. Wang, H. Liu, Phase transitions in a holographic superfluid model with non-linear electrodynamics, *Eur. Phys. J. C* 85 (2025) 14712. [doi:10.1140/epjc/s10052-025-14712-x](#).
- [27] M. Born, L. Infeld, Foundations of the new field theory, *Proc. Roy. Soc. Lond. A* 144 (1934) 425–451. [doi:10.1098/rspa.1934.0059](#).
- [28] T. Albash, C. V. Johnson, A Holographic Superconductor in the Presence of a Magnetic Field (2009). [arXiv:0901.4949](#).
- [29] R. Gregory, S. Kanno, J. Soda, Holographic superconductors with higher order corrections, *JHEP* 10 (2009) 010. [arXiv:0907.3203](#), [doi:10.1088/1126-6708/2009/10/010](#).
- [30] I. R. Klebanov, E. Witten, AdS / CFT correspondence and symmetry breaking, *Nucl. Phys. B* 556 (1999) 89–114. [arXiv:hep-th/9905104](#), [doi:10.1016/S0550-3213\(99\)00387-9](#).
- [31] P. Breitenlohner, D. Z. Freedman, Stability in gauged extended supergravity, *Annals Phys.* 144 (1982) 249. [doi:10.1016/0003-4916\(82\)90116-6](#).